LBID-2497

# Proposal for an Enhanced SASE X-ray FEL *

Alexander Zholents
Lawrence Berkeley National Laboratory
University of California,
Berkeley, California 94720

February 2004

Submitted to Phys. Rev. Lett.

* This work was supported by the Director, Office of Science, Office of High Energy and Nuclear Physics, High Energy Physics Division, of the U. S. Department of Energy, under Contract No. DE-AC03-76SF00098.

# Proposal for an Enhanced SASE X-ray FEL

Alexander A. Zholents
Lawrence Berkeley National Laboratory
University of California,
Berkeley, California 94720

ABSTRACT

We describe a technique by which an energy modulation of electrons via interaction with a laser pulse in a wiggler magnet prior entering a long SASE FEL undulator is used for a significant increase of the electron peak current. This results in a reduction of the gain length for the SASE process and a modification of the structure of the output x-ray radiation. It also temporally links the output x-ray pulse to the initial laser pulse, thus providing an opportunity for accurate synchronization between the visible pump pulse and x-ray probe pulse for pump-probe experiments.

PACS numbers: 41.50.+h, 41.60.Cr, 42.55.Vc, 52.59.-f

The technique of Self-Amplified Spontaneous Emission (SASE) (see [1] and references therein ) is a widely acknowledged tool for a production of an intense flux of photons with several keV photon energies. Two x-ray SASE Free Electron Laser (FEL) projects are already in an advanced stage [2]. In this Letter we propose a significant enhancement of the electron peak current entering the SASE FEL by using a conventional optical laser and demonstrate that this enchancement leads to a considerable reduction of the FEL gain length. The timing and duration of the x-ray pulse is also controlled by the timing and duration of the optical laser pulse, which makes pump-probe experiments available to the SASE FEL with potentially absolute temporal synchronization. Recent success in the production of VUV x-ray pulses of an attosecond duration [3-5] has inspired various proposals for a production of: i) soft and hard x-ray attosecond pulses using ponderomotive laser acceleration [6] or SASE and harmonic cascade FELs [7-9], ii) attosecond electron pulses [10]. With our scheme we could also produce a few hundred attosecond, solitary x-ray pulse.

Figure 1 shows a schematic of the proposed technique, which we call Enhanced SASE or ESASE. On the left the electron beam passes the linac and enters a wiggler magnet. At the same time a short ~ 50 fs optical laser pulse enters the wiggler and propagates through the wiggler at a small angle $\varphi$. The wiggler period $\lambda_w$ and wiggler parameter $K_w = eB_w\lambda_w / 2\pi mc^2$, where $m, e$ are the electron mass and charge, $c$ is the speed of light and $B_w$ is the peak magnetic field, are chosen such that $\lambda_L = \lambda_w\left[1 + K_w^2/2 + (\gamma_w\varphi)^2/2\right]/2\gamma_w^2$, where $\lambda_L$ is the laser wavelength and $\gamma_w$ is the relativistic factor for the average electron beam energy in the wiggler. Alternatively, it is possible to position the wiggler off-axis in an isochronous magnetic chicane and propagate the laser co-linearly with the electrons. The laser pulse overlaps only a short longitudinal section of the electron beam in the wiggler. For convenience we call this

section the *working section* (WS). Electrons in the WS interact with the laser field and emerge from the wiggler with energy modulation. The peak power of the laser field is chosen such that the amplitude of energy modulation significantly exceeds the uncorrelated energy spread of the electrons $\sigma_{\gamma 0}$. Next, the electron beam enters a second linear accelerator and gain energy to reach the final relativistic factor $\gamma_x$. This acceleration does not affect the energy modulation introduced in the wiggler and does not produce noticeable relative longitudinal motion of electrons because of the ultra-relativistic electron energies. Following acceleration the electron beam passes through a dispersive magnetic chicane where higher energy electrons travel a shorter path and lower energy electrons travel a longer path. This produces micro-bunching of the electrons in the WS and periodic enhancement of the electron peak current. As an illustration, Figure 2a shows the longitudinal phase space of the electrons after the chicane in a short segment within one laser wavelength.

Finally electrons enter a long undulator with period $\lambda_u$ and undulator parameter $K_x = eB_x\lambda_u / 2\pi mc^2$, where $B_x$ is the peak magnetic field, matched to produce radiation at the x-ray wavelength $\lambda_x = \lambda_u\left(1 + K_x^2/2\right)/2\gamma_x^2$ via the standard SASE process.

To simplify the analysis of the above described scheme we consider a rectangular optical laser pulse with a peak power $P_L$. Generalization to a Gaussian pulse shape is straightforward. The amplitude of the electron energy gain/loss in the wiggler $\Delta\gamma_w$ can be calculated by integration of electron interaction with the laser field along its trajectory in the wiggler. When the Rayleigh length of the laser beam equals approximately one quarter length of the wiggler and the electron beam size including wiggles of the electron beam trajectory is smaller than the laser beam spot size at the focus, then [11]:

$$\Delta\gamma_w^2 = 33\pi\frac{P_L}{P_A}N_w\xi_w\left(J_0\left(\xi_w/2\right) - J_1\left(\xi_w/2\right)\right)^2 \ , \qquad (1)$$

where $P_A = I_A mc^2/e \approx 8.7$ GW, $I_A$=17 kA is the Alfvén current, $\xi_w = K_w^2/\left(2 + K_w^2\right)$, and $J_0, J_1$ are the zero and first order Bessel functions of the first kind. $N_w$ is the number of wiggler periods chosen either smaller than the number of cycles in the laser pulse or such as to comply with an approximate condition of validity for the above formula, namely $N_w\Delta\gamma_w/\gamma_w \le 0.05$.

Following [12], the standard 1D FEL particle equations in the zero gain limit may be written as:

$$\frac{d\nu}{dz_*} = -\Omega^2\sin\theta \quad \text{and} \quad \frac{d\theta}{dz_*} = 2\pi\nu \qquad (2)$$

where $z_* \equiv z/L_u$ is the dimensionless length along the undulator, $\theta$ is the electron phase relative to the ponderomotive well, $\nu \equiv 2N_w\left(\gamma - \gamma_w\right)/\gamma_w$, and $\Omega^2 \equiv 2N_w\Delta\gamma_w/\gamma_w$ is the FEL-equivalent synchrotron tune. Using perturbation expansion of $\nu$ and $\theta$ in powers of $\Omega^2$<1, one obtains at the end of the undulator ($z_*$=1) through order $\Omega^2$ (see also [12,8]):

$$\nu_f = \nu_0 + \frac{\Omega^2}{2\pi\nu_0}\left[\cos(\theta_0 + 2\pi\nu_0) - \cos\theta_0\right]$$
$$\theta_f = \theta_0 + 2\pi\nu_0 + \frac{\Omega^2}{\nu_0}\left[\frac{\sin(\theta_0 + 2\pi\nu_0) - \sin\theta_0}{2\pi\nu_0} - \cos\theta_0\right] \quad (3)$$

where $\nu_0$ and $\theta_0$ refer to values at the wiggler entrance.

Following interaction with the laser beam in the wiggler, the electron beam is accelerated to energy $\gamma_x$ and passes through a magnetic chicane with a time-of-flight parameter $R_{56}$. We neglect relative longitudinal motions of the electrons during the acceleration, but consider them in the chicane. Although the laser is not present at this point it is still convenient to use the electron phase relative to ponderomotive well as a definition of electron location in the longitudinal direction. A new phase can be found from the following equation (see also [8]):

$$\theta_e = \theta_0 + C + 2\pi\nu_0(2\alpha+1) - \pi\Omega^2\left[(2\alpha+1)\frac{\sin\pi\nu_0}{\pi\nu_0}\sin\tilde{\theta} - \frac{1}{\pi\nu_0}\left(\frac{\sin\pi\nu_0}{\pi\nu_0} - \cos\pi\nu_0\right)\cos\tilde{\theta}\right] \quad (4)$$

where $\tilde{\theta} \equiv \theta_0 + \pi\nu_0$, $\alpha \equiv R_{56}\gamma_w / 2N_w\lambda_L\gamma_x$, and $C$ is an energy independent path-length difference term. Using (4) and presuming a uniform distribution of electrons in $\theta_0$ and a Gaussian distribution in $\nu_0$ with rms value $\sigma_\nu \equiv 2N_w\sigma_{\gamma 0}/\gamma_w$, one obtains the following expression for a WS electron current after the chicane (see also [13]):

$$I(z)/I_0 = 1 + 2\sum_{n=1}^{\infty} J_n\left(n\pi\Omega^2(2\alpha+1)\right)\mathrm{e}^{-\left(n\pi\Omega^2(2\alpha+1)/B\right)^2/2}\cos(nkz) \quad (5)$$

where $I_0$ is the electron current outside of the WS, $B = \Delta\gamma_w/\sigma_{\gamma 0}$, and $k = 2\pi/\lambda_L$. Note that high harmonics with $n > n_c = \sqrt{2}B/\pi\Omega^2(2\alpha+1)$ practically do not contribute to the sum in (5). For $n >> 1$, $J_n(nx)$ reaches maximum at $x \approx 1 + 0.809n^{-2/3}$ [14]. We use this fact and the above definition for $n_c$ to obtain an empirical value for $\pi\Omega^2(2\alpha+1) \approx 1 + 1/(4 + B/4)$ that maximizes $I(z)/I_0$. The right hand side of Eq.5 is a Fourier expansion of the periodic series of peaks spaced at $\lambda_L$ with each peak being approximated by the expression:

$$I(z)/I_0 = \mathrm{e}aB/\left(1 + (4Bz/\lambda_L)^2\right) \text{ with } a = 1/\left(1 + B^{1/\mathrm{e}}\right) \quad (6)$$

where $\mathrm{e} = 2.718$ is the base of the natural logarithm and $|z| < \lambda_L/2$. Thus the micro-bunch width is $\Delta z_0 = \lambda_L/2B$.

The increase of WS current is accompanied with a corresponding increase in the energy spread of electrons. Figure 2b shows the energy distribution of electrons taken at three positions along the compressed micro-bunch, marked as a,b,c in Figure 2a. Although the distribution functions in Figure 2b are not Gaussian, we still use the rms values of these to characterize the variation of the uncorrelated energy spread of electrons as a function of $z$ near the current peak in the WS using the following empirical formula:

$$\sigma_\gamma(z)/\sigma_{\gamma 0} = 1 + aB\left\{\mathrm{erf}\left(4z/\left(\Delta z_0 B^{1/8}\right) + \pi\right) - \mathrm{erf}\left(4z/\left(\Delta z_0 B^{1/8}\right) - \pi\right)\right\} \quad (7)$$

where $\mathrm{erf}(\mathrm{x})$ is the error function and $|z| < \lambda_L / 2$.

Finally, the electron beam goes through a long undulator where electrons micro-bunched at the optical wavelength within the WS produce enhanced SASE. The electrons outside of the WS also produce SASE, but have a much longer gain length because of their smaller current. We show later that it takes ~ 8 amplitude gain lengths for SASE to reach saturation, *i.e.* approximately $8\hat{M}_G$ undulator periods, where $\hat{M}_G$ is the gain length expressed in the number of undulator periods at the maximum of the current peak defined by Eq.6. Thus, to avoid gain degradation due to the slippage of electrons relative to the light in the undulator, the micro-bunch in the WS should have a sufficient length to support SASE until the very last gain length, i.e. $\Delta z_0 \geq 8\hat{M}_G \lambda_x$. This condition constrains the choice of the optical laser wavelength for a given $\lambda_x$: $\lambda_L / \lambda_x \geq 16\hat{M}_G B$.

We recall that the SASE output from a micro-bunch with a finite length $\Delta z_0$ becomes temporally coherent and nearly Fourier transform limited when $\Delta z_0 \leq 2\pi\hat{M}_G \lambda_x$ as estimated in [15]. This is remarkably close to the lower limit for a required micro-bunch length defined by slippage. Thus, it is fairly reasonable to expect in our scheme to have a nearly temporal coherent and Fourier transform limited x-ray micro-pulse produced by each individual micro-bunch. However, because of the SASE process, the carrier phase of the x-ray wave is not stable and changes randomly from one micro-pulse to the next.

Because of the micro-structure of the electron beam, the x-ray signal from undulator will appear as a progression of $N_w$ x-ray micro-pulses separated by $\lambda_L$. The upper estimate for a FWHM duration of each x-ray micro-pulse can be written as:

$$\Delta\tau \approx \left(\Delta z_0 / \sqrt{2}\mathrm{Ln}8 + \hat{M}_G \lambda_x\right)/c \approx 4\hat{M}_G \lambda_x / c \qquad (8)$$

where the first term in the right hand side shows the width of the electron current micro-pulse narrowed over the eight gain lengths and the second term shows pulse broadening by slippage in the undulator. The x-ray radiation produced by electrons outside of the WS has significantly less intensity because of the longer gain length at a significantly lower peak current. Thus, there is an absolute synchronization between the chain of the output x-ray micro-pulses and the laser pulse since only electrons from the WS, *i.e.* from the region that experienced interaction with the laser, produce intense x-ray signal. This feature can be used in pump-probe experiments with the x-ray pulse being a probe and a laser pulse or any other signal derived from laser pulse being a pump source. Moreover by changing the duration of the laser pulse and adjusting the number of active wiggler periods one can regulate the length of the WS and therefore the duration of the x-ray output. We will return to this feature later in a discussion of the generation of the intense attosecond x-ray pulses.

For illustration of the above described technique we present calculations made for the LCLS [2]. We use the following electron beam parameters: beam energy of 14.35 GeV, normalized emittance of 1.2 mm-mrad, $\sigma_{\gamma o} / \gamma_x = 0.8\mathrm{x}10^{-4}$, $I_0$ =3.4 kA, and consider a TOPAS laser [16] with $\lambda_L$ =2200 nm and $P_L \sim 6$ GW for energy modulation. In this illustration we choose to energy modulate the electrons at 2 GeV and consider a wiggler magnet with 10 periods, $\lambda_w$ =16 cm, and $K_w$ = 29 (peak magnetic field ~2 T). We note that energy modulation at a low energy is more convenient than at high energy

because of the greater length of the wiggler magnet required at higher energy. However if a wiggler magnet with just one or two periods is the goal, as is in the application considered later, then the energy modulation at the end of the linac can be an option. An additional advantage from energy modulation at a low energy is the small energy spread induced in the electron beam by the wiggler magnet itself.

From Eq.(1) we obtain $\Delta\gamma_w / \gamma_x$=6.4x10$^{-4}$ and $B$=8. Using Eq's (6,7) we plot $I(z)/I_0$ and $\sigma_\gamma(z)/\sigma_{\gamma 0}$ in Figure 3.

Finally, we consider the SASE process in the undulator with $\lambda_u$=3 cm and $K_x$=3.7 producing x-ray radiation at $\lambda_x$=0.15 nm. From the fitting formula of Ref.17 we found that the beta-function $\beta \approx$ 6 m yields the shortest amplitude gain length with $\hat{M}_G \cong 115$.[1] Then we calculate $M_G(z)$ for various pairs of $I(z), \sigma_\gamma(z)$ near the peak of the micro-bunch intensity and plot it in Figure 4. We note that the gain length everywhere outside of the WS calculated for a nominal electron beam parameters without enhancement in the electron current is almost 2.5 times longer.

We estimate the initial micro-bunching at $\lambda_x$=0.15 nm wavelength (not to be confused with micro-bunching at 2200 nm discussed previously) from a shot noise: $b_0 = \sqrt{ec/9I_0 eaB\hat{M}_G\lambda_x} \approx$ 1.5x10$^{-4}$ and calculate that approximately eight gain lengths will be needed to reach saturation with an assumed maximum bunching $b$=0.5. Then, using Eq.8, we find that the pulse duration for a single micro-pulse $\Delta\tau \approx$230 attosecond.

Finally we estimate the peak power at saturation $P_0 \approx$230 GW using the fitting formula from Ref.18: $P_0 \approx P_{\text{beam}}/8\pi\hat{M}_G$, where $P_{\text{beam}}$ is the beam power. The average power over the entire sequence of the x-ray micro-pulses is smaller by a duty factor $\lambda_L / c\Delta\tau \approx 30$.

The above discussed technique can also be used for a generation of attosecond x-ray pulses. Similar to Ref.8, one can employ interaction of electrons with a few-cycle 800 nm Ti:Sapphire laser pulse in a short wiggler. Laser pulses with 3.8 fs FWHM in intensity and stabilized carrier phase wave have been demonstrated [19]. Such a pulse with ~0.2 mJ pulse energy (not yet demonstrated) interacting with electrons in the wiggler magnet with just two periods will produce energy modulation shown in Figure 5. Here the central maximum is approximately 1.5 times higher than two nearest peaks. This causes the gain length for the smaller peaks to be approximately 14% longer. After eight gain lengths this small difference results in an output signal where the radiation coming from the central peak dominates the radiation coming from neighboring peaks. The radiation coming from the rest of the electrons is also insignificant because of their much longer gain length. All these effects allow a selection of the radiation from a solitary x-ray micro-pulse, which is in the above example, has an approximate width of 230 attosecond (FWHM).

In summary, we have demonstrated that electron peak current can be significantly increased by interaction of the electron beam with a high peak power laser pulse in a wiggler magnet prior to entering a SASE FEL. This shortens the FEL gain length and increases the peak power of x-ray radiation which comes out from the FEL as a sequence

---

[1] An increase of the beta-function to 12 m only marginally increases the gain length to $\hat{M}_G \cong$ 130.

of x-ray micro-pulses. Each micro-pulse in this sequence is nearly temporally coherent and Fourier transform limited and has width on the order of few hundred attoseconds. However, the carrier phase of the x-ray wave is not stable and changes randomly from one micro-pulse to the next. The duration of the entire sequence of micro-pulses can be controlled by adjusting the duration of the optical laser pulse and the number of active wiggler periods. In effect it can be made as short as a single micro-pulse by employing a few cycle laser pulse and a wiggler magnet with two periods. There is an absolute synchronization between laser pulse and the x-ray signal, which can be used in pump-probe experiments. Finally, the average x-ray power over the entire sequence of micro-pulses is also high and comparable to the average power in the present LCLS design.

We have not addressed possible problems related to the propagation of the electron micro-bunches with a high peak current through the undulator with a narrow-gap vacuum chamber deferring them to forthcoming publications.

Useful discussions with J.Corlett, P.Emma, W.Fawley, Z.Huang, G.Penn, J.Wurtele, and M.Zolotorev are gratefully acknowledged.

References

[1] C.Pellegrini, *NIM A*, **475**, 1 (2001).
[2] See, *e.g*., "Linac Coherent Light Source Design Study Report", *SLAC-R-521* (1998); "Tesla Technical Design Report", *DESY 2001-011* (2001).
[3] M.Hentchel et *al*., *Nature*, **416**, 509 (2001).
[4] M.Drescher et *al*., *Nature*, **419**, 803 (2002).
[5] R.Kienberger et *al*., *Nature*, **427**, 817 (2004).
[6] M.Zolotorev, *NIM A*, **483**, p.445 (2002).
[7] E.L.Saldin, E.A.Schneidmiller, and M.V.Yurkov, *Opt. Comm*., **212**, 377 (2002).
[8] A.A.Zholents, W.M. Fawley, *to be published in PRL*; *LBNL-54084Ext*, (2003).
[9] E.L.Saldin, E.A.Schneidmiller, and M.V.Yurkov, *DESY 04-013*, (2004), *submitted to Opt. Comm.*
[10] A.A.Zholents, W.Wan, and M.Zolotorev, PAC2001, 723, (2001).
[11] W.B.Colson, P.Elleaume, *Appl. Phys.,* **B54**, 101 (1982).
[12] W.Colson, Chap. 5 in *Laser Handbook*, Vol.6, North-Holland (1990); J.B.Murphy and C.Pelligrini, Chap.2, *ibid*.
[13] N.A.Vinokurov and A.N.Skrinsky, *Preprint INP 78-88*, Novosibirsk (1978).
[14] M.Abromowitz, I.Stegun, *Handbook of Mathematical Formulae*, (1964).
[15] R.Bonifacio et *al*., *Phys. Rev. Lett*., **73**, 70 (1994).
[16] Quantronix Scientific*, Tech. spec.,* www.quantronixlasers.com
[17] M.Xie, *NIM A*, **445**, 59 (2000).
[18] K.-J.Kim, M.Xie, *NIM A*, **331**, 1530 (1993).
[19] B. Schenkel et*. al. , Opt. Lett*, **28**, 1987 (2003).

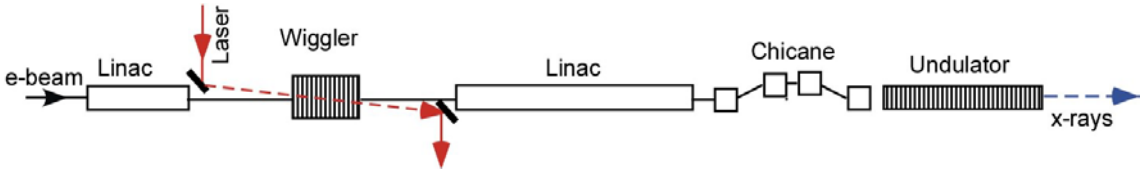


Figure 1. (Color) A schematic of ESASE x-ray FEL.

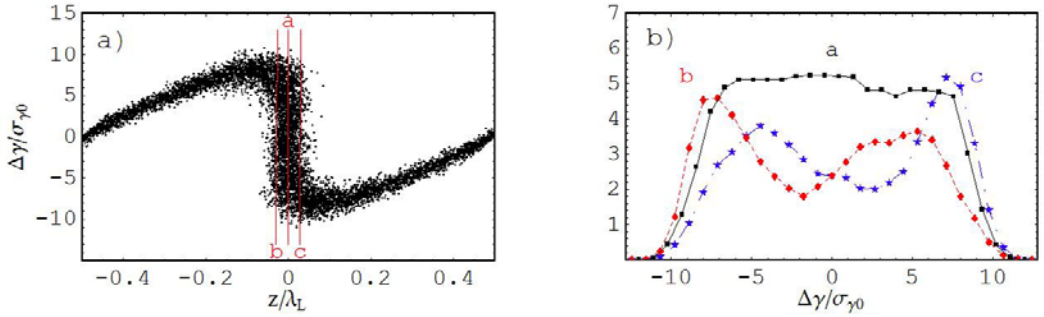


Figure 2 (Color) a) Longitudinal phase space after the chicane showing microbunching of electrons and an enhanced electron density. Only a part of the WS equivalent to one optical cycle at the laser wavelength is actually shown. b) The histograms of the energy distribution of electrons after the chicane taken along the lines a,b,c in Figure 2a.

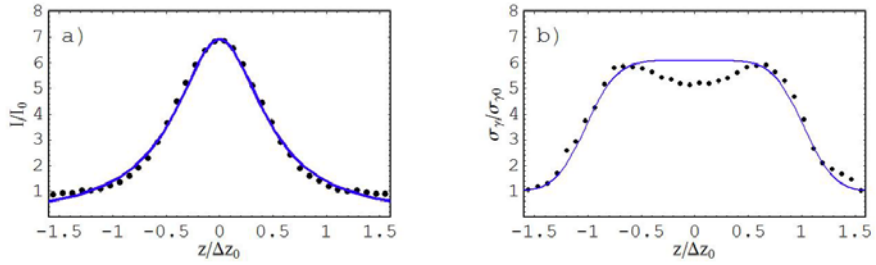


Figure 3 (Color) Normalized peak current a) and energy spread b) versus distance within the micro-bunch. Dots show computer simulation results while the solid line was obtained with Eq.s 6 and 7.

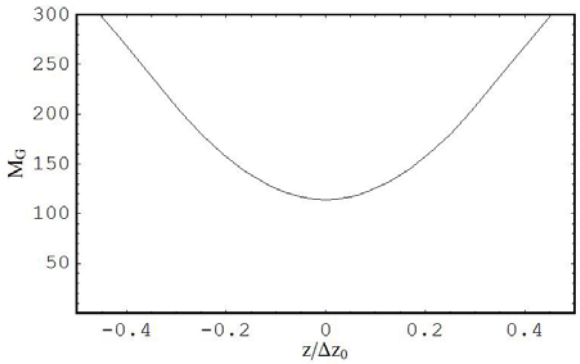


Figure 4. Gain length at various distances within the micro-bunch calculated using fitting formula from Ref.17.

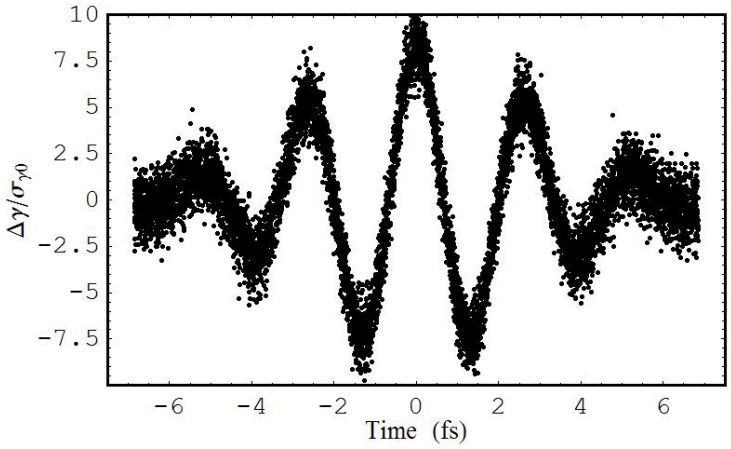


Figure 5. Energy modulation produced in interaction with a few-cycle laser pulse.